The Effect of Impurities on the Steam Reforming of Ethanol over Ruthenium/Alumina

Journal:	*Catalysis Science & Technology*
Manuscript ID:	CY-ART-04-2014-000560.R1
Article Type:	Paper
Date Submitted by the Author:	03-Jun-2014
Complete List of Authors:	Jackson, S; University of Glasgow, Department of Chemistry Bilal, Muhammad; University of Glasgow, Chemistry

The Effect of Impurities on the Steam Reforming of Ethanol over Ruthenium/Alumina.

Muhammad Bilal and S David Jackson*

Centre for Catalysis Research, WestCHEM, School of Chemistry, University of Glasgow, Glasgow G12 8QQ, Scotland, UK

* Author to whom all correspondence should be addressed

Abstract

Steam reforming of bioethanol is a promising route for H_2 production. However, the presence of impurities in technical bioethanol has a significant influence on the activity and lifetime of the catalyst. Therefore, the aim of this project was to study the influence of C_3-impurities (1-propanol, 2-propanol (IPA), propanal, acetone and propyl amine) on the steam reforming of ethanol over Ru/Al_2O_3 at 773 K and 20barg. It was found that the addition of C_3-alcohols significantly decreased the conversion of ethanol and increased the rate of catalyst deactivation. This deactivation of the catalyst in the presence of C_3-alcohols was attributed to high olefin formation and incomplete decomposition of the C_3-alcohols, which resulted in coke formation over the catalyst. In contrast propyl amine and acetone addition maintained high ethanol conversion throughout the time on stream. However analysis of the product distribution suggested that the main reaction was ethanol decomposition taking place over the support and that the metal was completely deactivated for steam reforming. The addition of acetone to ethanol also significantly changed the nature of coke from graphitic to amorphous carbon. The addition of propanal resulted in behaviour initial akin to propanol but eventually moved to selectivity similar to that found with acetone.

Key words: Ethanol, impurities, steam reforming, ruthenium

Introduction

Hydrogen was first discovered in 1766 by Henry Cavendish (1731-1810) in London, when he collected it over a metal and described it as "inflammable air" [1]. It is the lightest and most abundant element (making up over 90% of the atoms in our universe) and although in the earth's atmosphere it is present at very low levels (0.1 ppm) in a pure form, more than 50% of our surroundings contain hydrogen present in a combined form with other elements [2]. Currently hydrogen is used as a chemical in the synthesis of ammonia and methanol, hydrotreating, of petroleum feedstocks to remove sulphur and nitrogen, hydrogenation of unsaturated hydrocarbons and the reduction of organic and inorganic compounds [3]. However, due to the development of the fuel cell technology, hydrogen demand is expected to increase to fulfil the requirement of future energy [4]. The total hydrogen production in the world is around 50 million metric tonnes produced principally by steam reforming of natural gas with much of the rest produced as a by-product hydrogen from petroleum refinery gases and other cracking operations [5].

Approximately 80% of the world's energy needs are met directly or indirectly from non-renewable sources such as fossil fuels [6, 7]. However, use of fossil fuels as a primary energy source has led to serious crises and environmental pollution on a global scale [8]. In order to mitigate environmental problems and reduce fossil fuel consumption, there has been an increased focus on generating fuel for transportation and hydrogen production from renewable sources [5]. Renewable sources for fuel, such as bioethanol, are biodegradable and non-toxic, free of sulphur and aromatics and produce less exhaust

emissions than fossils fuels [9]. Various efforts have been made to convert biomass to hydrogen for fuel cells [10] but in recent years the steam reforming of bioethanol has gained intense interest for the production of H_2 (see ref. 11 and references therein). The interest of researchers in ethanol steam reforming (ESR) may be due to the series of advantages of ethanol *i.e.* it is easier to store, handle and transport in a safe way due to low toxicity and volatility [12]. In addition the steam reforming of ethanol can yield up to 6 mol. hydrogen per mol. of ethanol. Bioethanol can be obtained from biomass by fermentation process which contains about 20 vol% of ethanol with water as the major components. Crops and vegetables consume carbon dioxide produced from the steam reforming of bioethanol, so the carbon cycle is closed and these carbon dioxide emissions are not considered to contribute to global warming [12]. Two types of bioethanol of exist; 1st generation bioethanol and 2nd generation bioethanol and the difference is in their origin. First generation bioethanol is produced from fermentation of sugar cane, corn and sugar beets whilst 2nd generation is obtained from wood, household waste and wheat straw [13]. Both generations of bioethanol contain different types of different organic functional group impurities, which have a significant effect on the steam reforming reactions and play an important role in the catalyst deactivation [14]. It is therefore necessary to remove impurities from bioethanol before using in the steam reforming reaction. However, according to Ladish *et al.* [15] 70-85% of energy used in bioethanol preparation is consumed during purification from different impurities. Therefore use of crude bioethanol for steam reforming will therefore minimize the process heat (steam) for the energy intensive distillation along with the capital cost of the distillation equipment [13]. The development of a catalyst for steam reforming of direct crude bioethanol, which has

ability to tolerate the different impurities present in bioethanol is of keen interest. Christensen and co-workers [13] reported that using a crude bioethanol will result in a faster catalyst deactivation because of the impurities but noted that the initial activity of the catalysts was not affected and suggested that the focus should be on catalyst lifetime rather than activity. Devianto *et al*. [16] also examined the effect of impurities on ethanol steam reforming and found that methanol and diethyl amine did not negatively affect activity whereas propanol and acetic acid resulted in catalyst deactivation. Duprez and co-workers [17] studied the effect of a range of impurities and found that the poisoning effect induced by impurities gave the following increasing order: diethylamine ~ butanal < no impurity < acetic acid < butanol < diethylether ~ ethyl acetate.

The aim of this study was therefore to follow on from our previous work [18] and investigate the effect of different impurities present in bioethanol on ESR over a Ru/Al_2O_3 catalyst using a model "bioethanol" containing 1 mol. % C-3 impurities such as 1-propanol, 2-propanol (IPA), propanal, acetone and propylamine. The addition of individual components gave a clear picture of how different functional groups affected catalyst activity and selectivity during the steam reforming of ethanol, while the use of a common carbon backbone for the impurities ensured that the effects were due to the functional group and not due to variations in the amount of carbon in the impurity. Post reaction characterisation of spent catalysts was carried out using various techniques to investigate the cause of catalyst deactivation during ESR. The reaction was carried out at 20 barg rather than atmospheric pressure. Although this potentially inhibits the steam reforming reaction it more closely mimics typical industrial steam reforming scenarios

where running the steam reforming reaction at pressure to deliver high pressure hydrogen is more efficient that subsequently compressing low pressure hydrogen. Our choice of ruthenium was influenced by the fact that it has been used as the active component in other studies and been shown to be one of the more active steam reforming metals [13, 19, 20].

Experimental

The catalyst used in this project was a 0.2 % Ru/Al_2O_3 catalyst prepared via incipient wetness impregnation using $Ru(NO)(NO_3)_3$. The alumina was characterised by XRD analysis to be a mixture of γ-and δ-alumina phases. After drying the catalysts were calcined at 723 K for 4 h and had a BET surface area of 104 m^2g^{-1}. From XRD the metal particle size was calculated at 12.5 nm after reduction in hydrogen at 873 K for 2 h, giving a dispersion of ~8.5 %. The catalysts were crushed to particle sizes between 600 to 425 μm and then used for ESR.

The ethanol (AnalaR Normapur, 99.99%), acetone (Fisher Scientific, 99.99%), IPA (Sigma Aldrich, 99.5%), 1-propanol (Alfa Aesar, 99.0%), propylamine (Sigma Aldrich, 99.0%) and propanal (Sigma Aldrich, 97.0%) were all used as received.

Ethanol steam reforming reactions were carried out in a continuous-flow, high-pressure, microreactor. Prior to reaction, catalysts (0.25 g) were reduced *in-situ* at 873 K for 2 hours using hydrogen gas at a flow rate of 50 ml min^{-1}. The hydrogen was then purged

from the system with argon and the temperature was decreased to 773 K (reaction temperature) simultaneously the total pressure in the apparatus was increased to 20 barg. The water-ethanol mixture was set to obtain a steam to ethanol molar ratio of 5:1 in the gas phase. The amount of each impurity added to water-ethanol mixture was 1 mol.% with respect to ethanol. The ethanol-water mixture was introduced to the reactor system through a vaporizer set at a temperature of 773 K. The gas flow rate of the steam/ethanol was set at 416.6 ml min^{-1}, which was generated by pumping the liquids through a Gilson pump at a rate of 0.412 ml min^{-1}. The argon gas flow rate was set at 10 ml min^{-1} achieving an overall GHSV of 50,000 h^{-1}. Once all the reaction parameters had been fixed, analysis was begun by flowing reactants from vaporizer to reactor. The eluant from the reactor tube in gaseous form entered a knockout pot where high boiling point products were liquefied and collected and analysed by a Trace GC-2000 Series using a Zebron column and FID detector. The temperature of the knockout pot was kept at 273 K. The gaseous products were analysed by an on-line Varian GC 3400 using a TCD detector and a carboxen^{Tm}1010 plot column. Each reaction was performed at 773 K for 100 hours time on stream. Mass balance in the system was ~100 %. The extent of carbon deposition as a function of the feed was < 1 %.

The amounts and nature of coke were determined by analysing post reaction catalyst samples using analytical techniques such as BET, powder XRD, Raman spectroscopy, SEM and TGA-DSC connected to a mass spectrometer for evolved gas analysis.

BET surface areas and pore volume of pre- and post-reaction catalysts were measured using a Micromeritics Gemini III 2375 Surface Area Analyser. Prior to analysis, between 0.04-0.05g of catalyst were placed into a vial and purged under a flow of N_2 (30ml min^{-1}) over night at 383 K to remove moisture and any physisorbed gases from the catalyst sample. Powder X-ray diffraction patterns of pre and post reaction samples were obtained using a Siemens D 5000 X-ray Diffractometer (40kV, 40mA, monochromatic). The scanning range was $5^o \leq 2\ \theta \leq 85^o$ with a scanning rate of 10 seconds per step and a step size of 0.02°. Raman spectra of post reaction catalysts were obtained with a Horiba Jobin Yvon LabRAM High Resolution spectrometer. A 532.17nm line of a coherent Kimmon IK series He-Cd laser was used as the excitation source for the laser. Laser light was focused for 10 seconds using a 50x objective lens and grating of 600. The scattered light was collected in a backscattering configuration and was detected using nitrogen cooled charge-coupled detector. A scanning range of between 100 and 4100 cm^{-1} was applied. SEM images of the post reaction catalysts were obtained using a Philips XL30 Environmental SEM. The sample was irradiated with a beam of electrons, this was followed by changing magnification and focusing for increasing resolution of the catalyst surface. TPO was carried out on post reaction samples using a combined TGA/DSC SDT Q600 thermal Analyser connected to an ESS Mass Spectrometer for evolved gas analysis. Each sample was heated from room temperature to 1000°C using a heating ramp of 5°C min^{-1} under 2% O_2/Argon gas at a flow rate of 100 ml min^{-1}.

Results

To the water/ethanol feedstream was added 1 mol.% of 1-propanol and in a separate experiment 1 mol.% propylamine. These modified feeds were passed over the alumina support at 773 K and 20 barg and compared to the behaviour when no impurity was present. The conversion observed is shown in Fig. 1, while the selectivities are reported in Table 1.

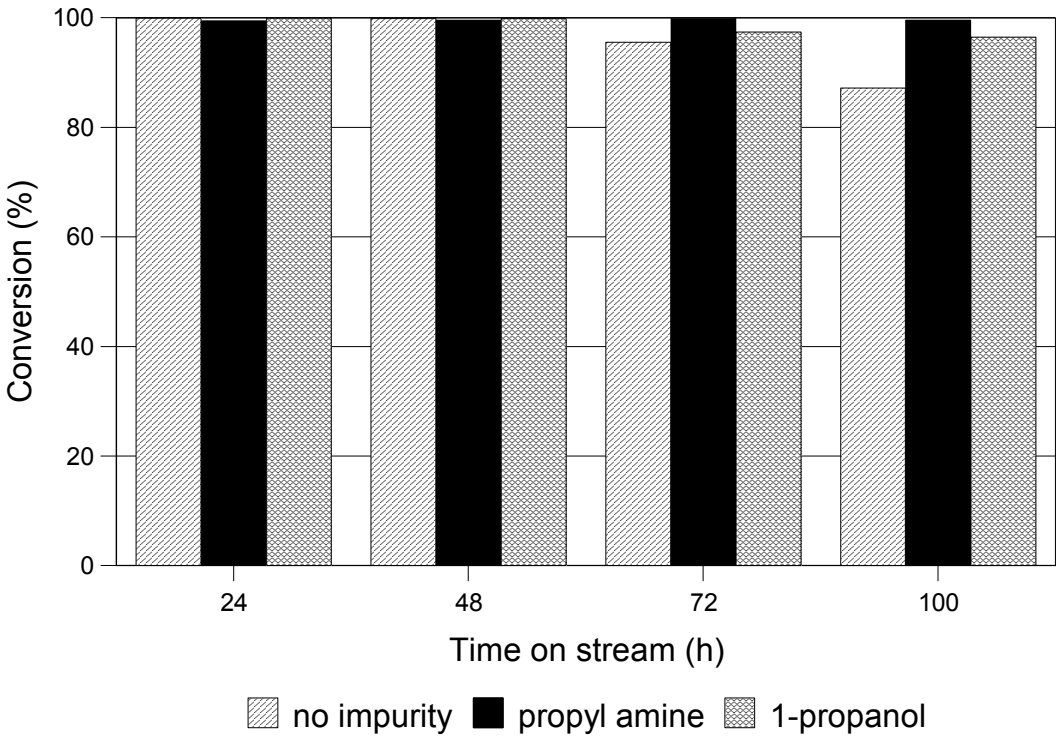

Figure 1. Conversion of ethanol over alumina at 773 K in the absence and presence of impurities. Conditions: 773 K, 20 barg, 5:1 water:ethanol, 1 % impurity.

Table 1. Dry gas selectivities[a] at 100 h TOS over the alumina support at 773 K.

Impurity	**Molar selectivity of dry gas (%)**					
	H_2	**CH_4**	**CO_2**	**CO**	**C_2H_4**	**C_2H_6**
No impurity	43	28	20	6	tr[b]	tr
1-Propanol	46	27	10	16	tr	tr
Propyl amine	48	26	17	9	tr	tr

a. dry gas selectivity is defined as moles of gas n_i/Σmoles of gas n_{1-i}

b. tr = trace, <0.5 %

The addition of a 1 mol.% impurity to the water/ethanol mixture had a significant effect on the conversion of ethanol over the Ru/Al_2O_3 catalyst at 773 K and 20 barg pressure as can be seen in Fig. 2. Up to 25 hours time on stream (TOS) the conversion of ethanol was higher in all the reactions containing an impurity than the pure ethanol reaction. However after 25 hrs TOS, a swift decrease in the ethanol conversion took place over the Ru/Al_2O_3 catalyst, when 1-propanol, propanal and IPA were the impurities, such that all these systems returned lower conversions of ethanol. In contrast the reactions where acetone and propylamine had been added showed higher conversion than ethanol, with no impurity added, for the whole TOS.

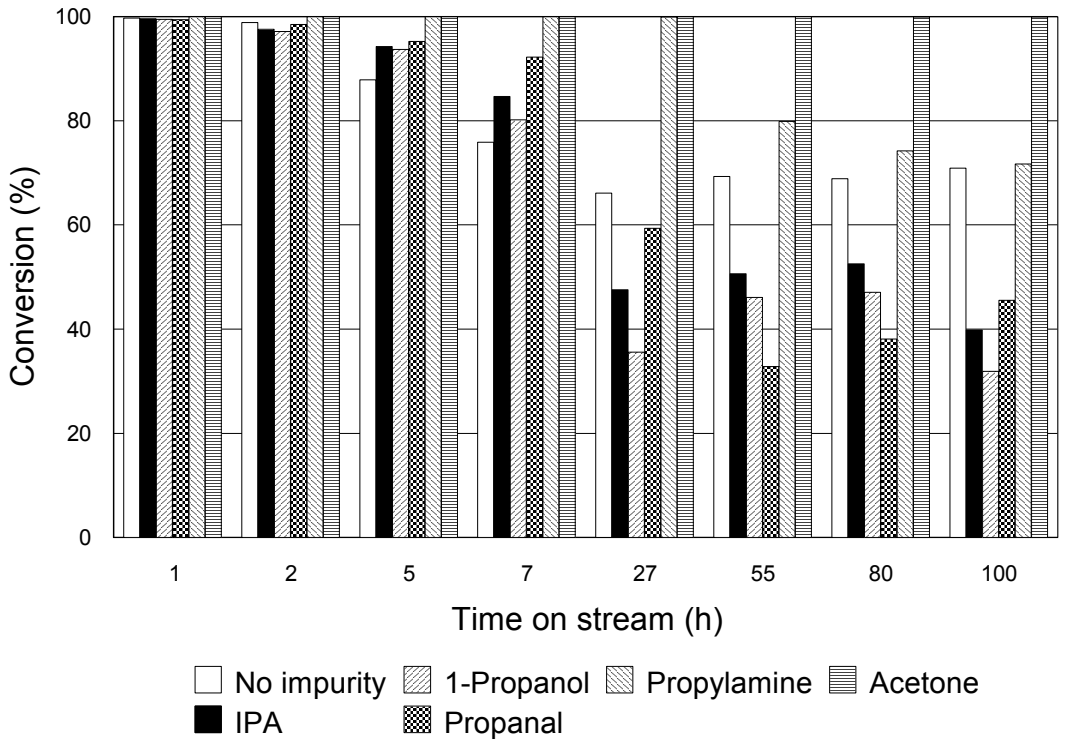

Figure 2. Conversion of ethanol over Ru/Al_2O_3 catalyst during the reaction with different impurities. Conditions: 773 K, 20 barg, 5:1 water:ethanol, 1 % impurity.

Table 2. Dry gas selectivities at 100 h TOS over Ru/alumina at 773 K.

Impurity	**Molar selectivity of dry gas (%)**					
	H_2	**C_2H_4**	**CO_2**	**CO**	**CH_4**	**C_2H_6**
No impurity	46	35	6	3	6	4
1-Propanol	57	24	7	3	6	3
IPA	61	21	7	3	6	2
Propanal	58	4	16	5	18	0
Propylamine	50	0	19	6	25	0
Acetone	44	3	15	11	27	0

Table 3. Hydrogen yield (mol.mol^{-1}) at 100 h TOS over Ru/alumina at 773 K.

Impurity	None	IPA	1-propanol	propanal	propylamine	acetone
H_2 yield	2.10	2.06	2.17	3.14	3.18	2.66

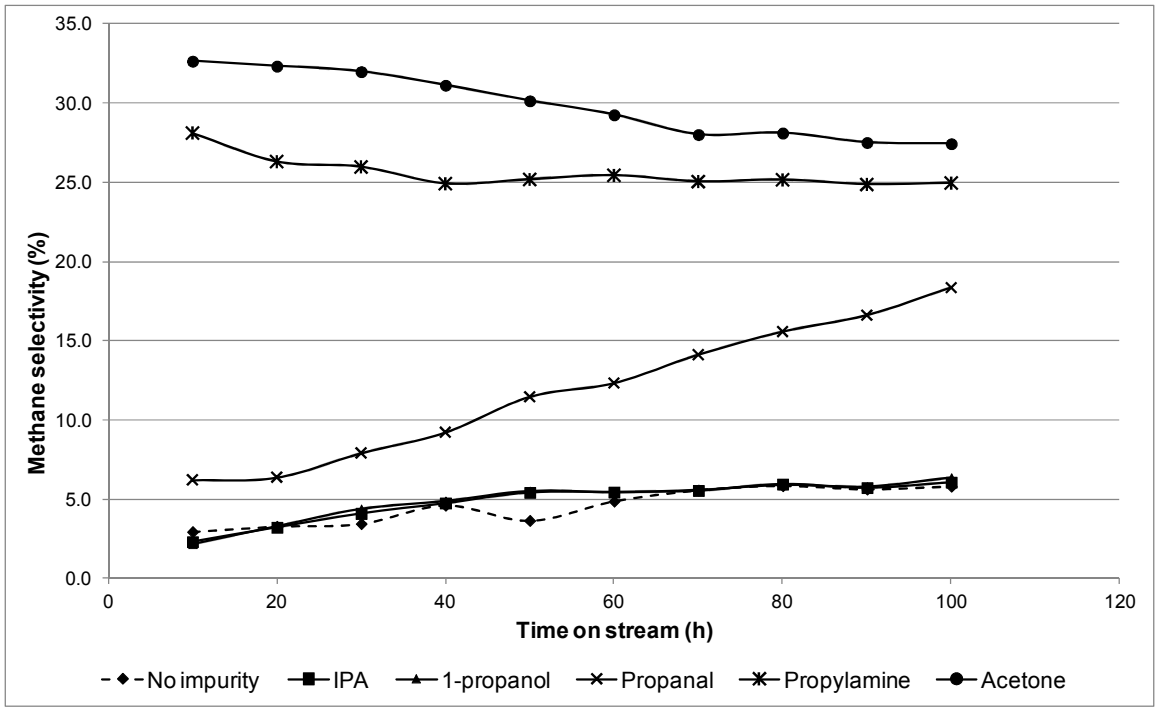

Figure 3. Methane selectivity as a function of time on stream for all systems. Conditions: 773 K, 20 barg, 5:1 water:ethanol, 1 % impurity.

The dry gas selectivities are reported in Table 2. It can be seen that the selectivities split into two groups, those with high ethene and low methane and those with low ethene and high methane. The behaviour of ethene and methane is shown against TOS in Figs. 3 and 4. The difference between the two groups can clearly be seen but it is also clear that the

system that has propanal as the impurity starts in the group with low methane and high ethene selectivity yet finishes in the group with low ethene and high methane selectivity.

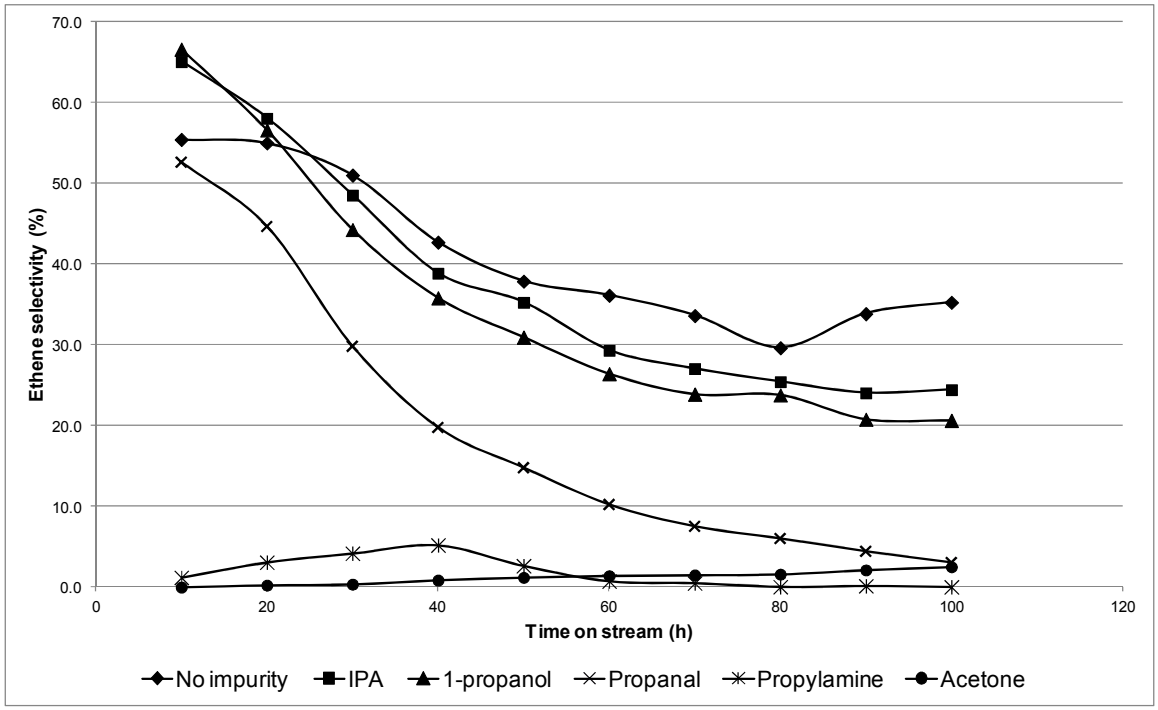

Figure 4. Ethene selectivity as a function of time on stream for all systems. Conditions: 773 K, 20 barg, 5:1 water:ethanol, 1 % impurity.

Liquid samples were collected and analysed as well as the gas phase; the data are reported in Table 4. Yields are calculated as (moles of product produced)/(mole ethanol fed)*100 %. Trace levels (< 0.1 %) of methanol and ethyl acetate were also detected with all reactions.

Table 4. Liquid phase product yields (mol.mol^{-1}). Conditions: 773 K, 20 barg, 100 h TOS, 5:1 water:ethanol, 1 % impurity.

	Yield (mol.mol^{-1} %)					
Impurity / Product	No impurity	1-propanol	IPA	propanal	propyl amine	acetone
Acetaldehyde	3.1	3.3	2.6	6.3	9.7	6.7
Diethyl ether	3.5	1.0	1.1	0.2	0.2	0
Acetone	1.2	1.3	0.9	1.6	2.9	8.3
Acetic acid	0.8	1.2	0.9	1.4	1.6	2.1
1,1-DEE	0.2	0.3	0.2	0.5	0	0

Spent catalyst samples from the pure ethanol reaction and all impurity reactions were analysed by TGA. The derivative weight profiles of temperature region 673 K – 1173 K are shown in Fig. 5: below 673 K and above 1173 K no significant change in weight was observed. The sole carbon containing species desorbed during the TGA was carbon dioxide. The carbon dioxide profile mirrored that of the derivative weight for all systems.

The crystallinity and nature of coke was determined by powder XRD and Raman spectroscopy. The powder XRD patterns shown in Fig. 6 indicate that the addition of impurities to ethanol has no effect on the catalyst morphology. However, a broad peak at 26^{o} 2θ position, which is a characteristic peak of graphitic carbon, significantly changed

with addition of different impurities to ethanol. When acetone was added as the impurity no peak for graphitic carbon was observed over the catalyst, whilst when 1-propanol was added as the impurity, the catalyst gave a similar peak to that of pure ethanol.

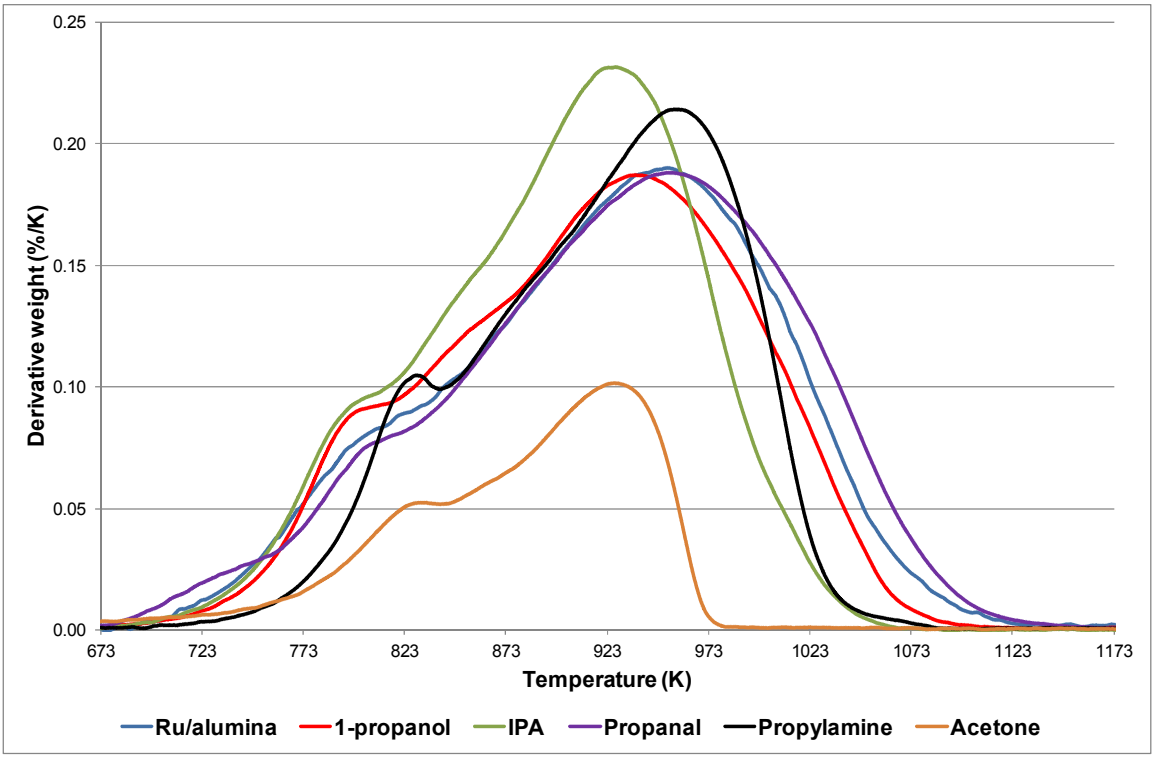

Figure 5. Derivative TGA weight profile of post reaction Ru/Al_2O_3 catalyst used with different impurities.

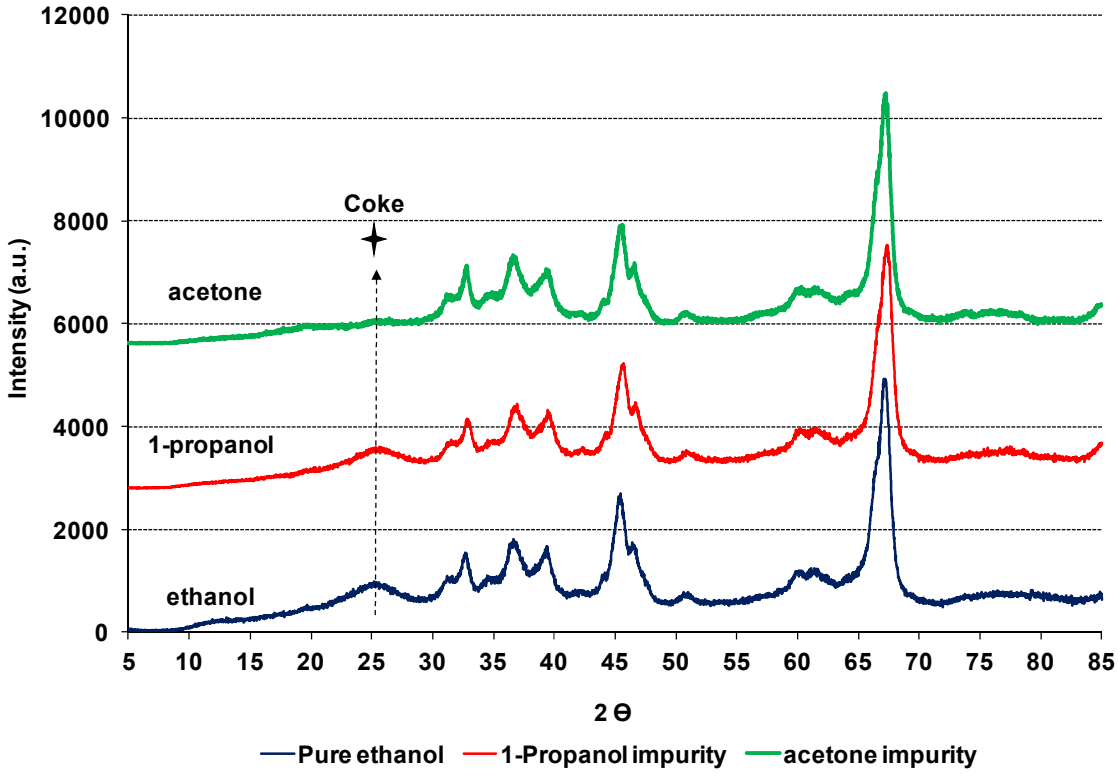

Figure 6. Powder XRD patterns for post reaction Ru/Al_2O_3 catalysts after use in ESR with no impurities, with 1-propanol as the impurity and with acetone as the impurity. (The powder XRD patterns are offset for clarity)

All the samples were analysed by Raman spectroscopy. Fig. 7 shows the spectra obtained from the catalysts used with pure ethanol, with 1-propanol as the impurity and with acetone as the impurity. All samples showed characteristic bands of graphitic carbon similar to those observed from the reaction with pure ethanol, except the catalyst that had been used with acetone as the impurity; with that catalyst no graphitic bands were observed. Similarly the ratio of the intensity of the D and G bands, which measure the disorder of graphitic carbon, varied slightly for different impurities as shown in Table 5.

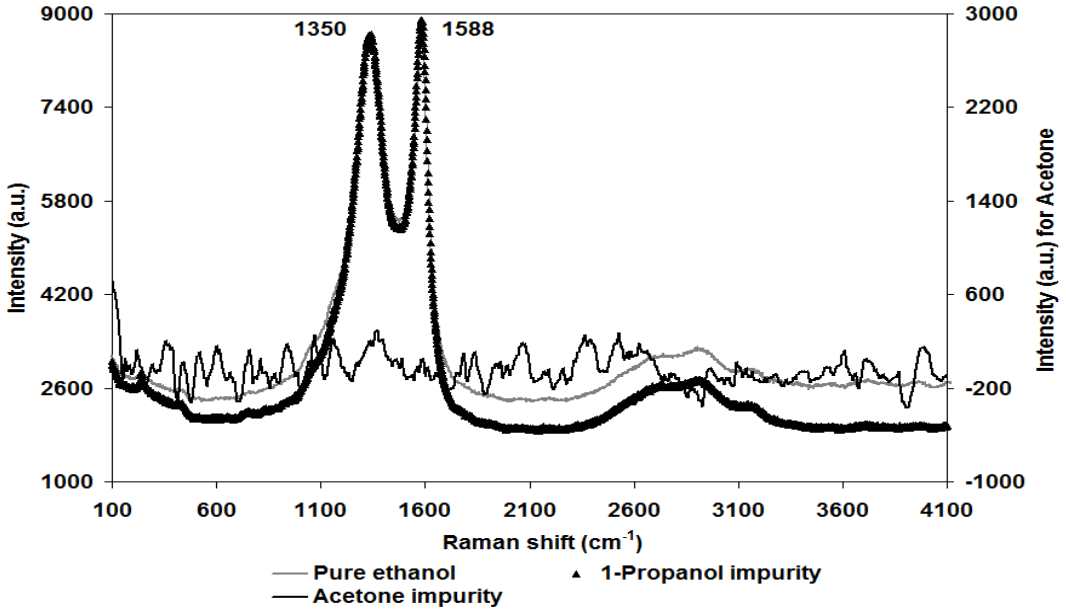

Figure 7. Raman spectra for post reaction Ru/Al_2O_3 catalysts after ESR of pure ethanol, with 1-propanol as an impurity and acetone as an impurity.

Impurity	BET Surface Area(m^2/g)	Pore Volume (cm^3/g)	Weight loss in TPO (%)	(I_D/I_G)
Reduced@600	100	0.43	-	-
No impurity	32	0.07	39	0.99
IPA	38	0.07	38	0.92
1-Propanol	36	0.07	38	0.99
Propanal	16	0.03	41	0.92
Propylamine	36	0.10	35	0.96
Acetone	50	0.20	19	-

Table 5. BET surface area, % weight loss and Raman band ratios over Ru/Al_2O_3 catalyst for reactions with different impurities.

The BET analysis shows that compared to the catalyst in reduced form the surface area and the pore volume of all the spent catalysts were significantly decreased. The decrease in the pore volume suggests that carbonaceous materials were mostly deposited in the pores of the catalyst. Table 5 illustrates that among the different impurities, the acetone impurity resulted in the highest surface area and pore volume due to the formation of the least amount of coke whilst the catalyst used with propanal as the impurity gave the lowest BET surface area due to the highest coke formation.

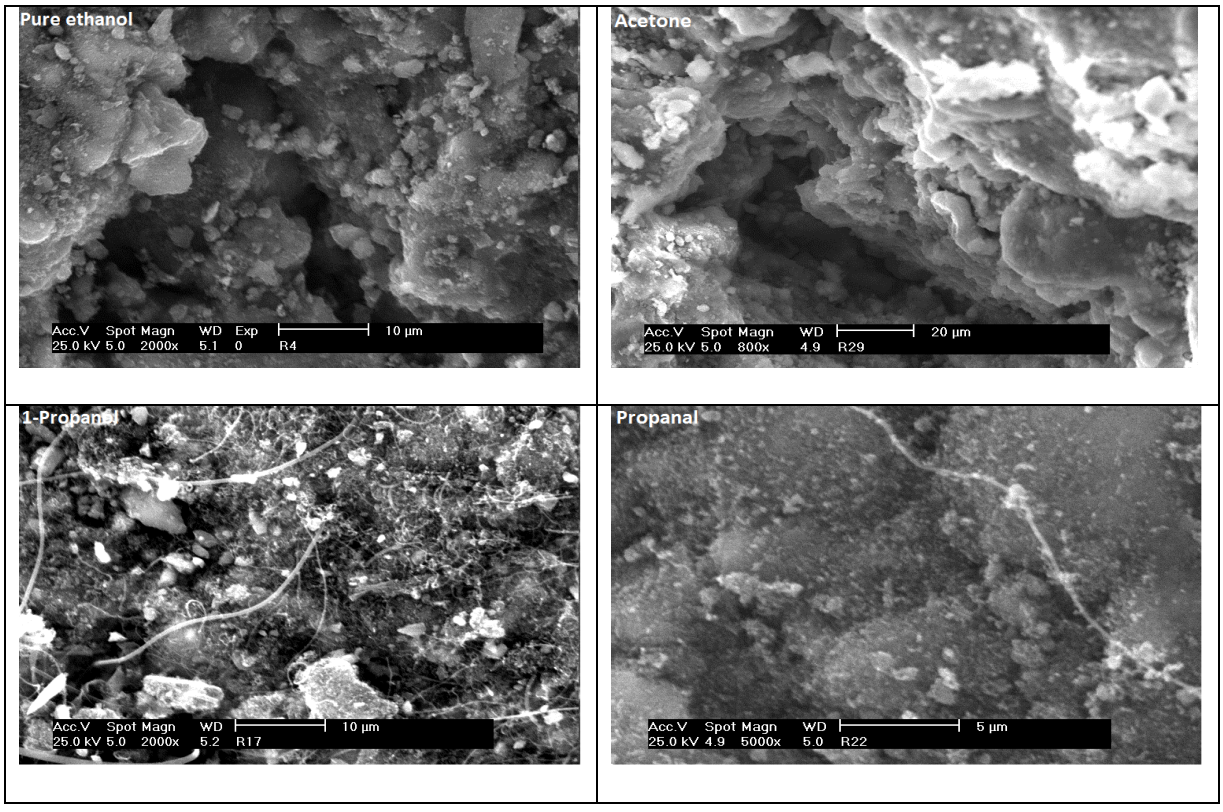

Figure 8. SEM images for post reaction Ru/Al_2O_3 catalyst of pure ethanol, 1-propanol, propanal and acetone impurity reactions

To study the catalyst morphology the spent catalysts were analysed by SEM. The SEM images show that no carbon nanotubes (CNTs) were observed when acetone was used as the impurity and the pure ethanol reaction as shown in Fig. 8. These results illustrate that in these reactions coke is deposited in an amorphous form. In contrast catalysts that had been used with 1-propanol and propanal as the impurities revealed a number of small CNTs. Both fibrous and small CNTs were detected when 1-propanol was the impurity. These results illustrate that besides amorphous carbon, CNTs are formed on these catalysts. Therefore the addition of 1mol% of 1-propanol and propanal impurities to ethanol significantly changed the morphology of coke with both amorphous coke and CNTs produced.

Discussion

The conversion of ethanol in the presence of different impurities shows that in a binary mixture, the conversion of one compound is significantly influenced by the presence of the other compound even at low concentrations. In a previous study [18] it was shown that alumina catalyses the ethanol decomposition reaction and the water gas shift reaction but not steam reforming. The results from the addition of 1-propanol and propyl amine to the ethanol show similar behaviour over the alumina support in that the product distributions confirm that the only reactions occurring are ethanol decomposition and WGS. For example the selectivity of the reaction with the 1-propanol additive can be described at 100 h by the following reactions:

$3C_2H_5OH \rightarrow 3CO + 3CH_4 + 3H_2$

$2CO + 2H_2O \rightarrow 2CO_2 + 2H_2$

Overall: $3C_2H_5OH + 2H_2O \rightarrow CO + 3CH_4 + 5H_2 + 2CO_2$

When the reactions with an impurity present are performed over the Ru/alumina catalyst it can be seen from Figs. 2 – 4 and Table 2 that the impurities fall into three groups, i) acetone and propyl amine that maintain a higher conversion than that found with pure ethanol but with a lower selectivity to hydrogen; ii) 1-propanol and IPA that reduce activity but show an increased selectivity to hydrogen; and iii) propanal which starts with a high selectivity to ethene but one that decreases over time. It is worthwhile noting that between 7 and 24 h all impurities result in higher conversion than that found with ethanol alone: it is only after 24 h on-stream that the differences become truly apparent. This behaviour is in agreement with the results of Christensen and co-workers [13], who saw little effect of impurities on initial activity. When the yield of hydrogen (Table 3) is considered however, in agreement with the work of Duprez and co-workers [17] and Devianto *et al*. [16] with diethyl amine, the experiments with propyl amine added as an impurity show the highest hydrogen yield.

The equilibrium mix for ethanol steam reforming at 773 K, 20 barg and a steam:ethanol ratio of 5 is 27 % hydrogen, 48 % methane, 24 % carbon dioxide and 1 % carbon monoxide: this is considerably different from the values observed experimentally. The low carbon monoxide and high methane and carbon dioxide levels are a reflection of a significant amount of methanation and water-gas shift (WGS), both of which are

favoured at lower temperatures. Experimentally the systems that come closest to the equilibrium mix are the alumina and the reaction that has acetone as the impurity. The difference from equilibrium can be related in these systems to a lack of methanation activity. In the case of the alumina, no metal is present to catalyse the methanation reaction and, as we shall see below, with the acetone impurity the metal function is rapidly deactivated. In both these systems the methane produced comes from ethanol decomposition.

Effect of 1-propanol and IPA

The poisoning effect of higher alcohols (1-propanol, IPA) has been observed previously, Rass *et al.* [13] used technical bioethanol and found that larger alcohols deactivated the catalyst severely. They found that carbon formation in technical bioethanol was slightly higher than from a pure ethanol/water mixture. However in our tests the quantity of carbon deposited, as measured by TPO (Table 5), was not greater than that obtained with pure ethanol. Interestingly it was found that conversion of the IPA impurity was high and no significant deactivation was observed in its conversion in comparison to that of ethanol. At these temperatures the dehydrogenation equilibrium between IPA and acetone lies in favour of acetone so it may be expected that the acetone yield would increase however the acetone yield is less than 1 %, which is less than that found in the absence of an impurity (Table 4). In agreement with that found by Devianto et al. [16] the conversion of 1-propanol followed that of ethanol, indicating a difference in reactivity between primary and secondary alcohols. Trane-Restrup *et al.* [21] also found that the

position of the oxygen functionality had an impact on reactivity. Nevertheless with 1-propanol and IPA as impurities the ESR system shows a high selectivity to ethene. The selectivities observed can be described by the following reactions:

for ESR with 1-propanol as the impurity,

$$5C_2H_5OH + 5H_2O \rightarrow 10CO + 20H_2$$

$$4CO + 12H_2 \rightarrow 4CH_4 + 4H_2O$$

$$4CO + 4H_2O \rightarrow 4CO_2 + 4H_2$$

$$18C_2H_5OH \rightarrow 18C_2H_4 + 18H_2O$$

$$2C_2H_4 + 2H_2 \rightarrow 2C_2H_6$$

Overall:

$$23C_2H_5OH + 5H_2O \rightarrow 2CO + 4CH_4 + 10H_2 + 4CO_2 + 16C_2H_4 + 2C_2H_6 + 18H_2O$$

while for ESR with IPA as the impurity,

$$8C_2H_5OH + 8H_2O \rightarrow 16CO + 32H_2$$

$$6CO + 18H_2 \rightarrow 6CH_4 + 6H_2O$$

$$7CO + 7H_2O \rightarrow 7CO_2 + 7H_2$$

$$23C_2H_5OH \rightarrow 23C_2H_4 + 23H_2O$$

$$2C_2H_4 + 2H_2 \rightarrow 2C_2H_6$$

Overall:

$$31C_2H_5OH + 9H_2O \rightarrow 3CO + 6CH_4 + 19H_2 + 7CO_2 + 21C_2H_4 + 2C_2H_6 + 23H_2O$$

However although these analyses do account for all carbon containing species they do not allow an accurate description of the hydrogen production. A slight correction can be applied by considering the carbon deposition process. From the XRD, SEM and Raman spectroscopy it is clear that much of the carbon produced is graphitic in nature with

CNTs also formed. These species are highly dehydrogenated and can liberate hydrogen during their synthesis. It is known that ethene can convert to pyrolytic coke over metal surfaces [22] hence assuming that ethene is a major route to coke we get,

$C_2H_4 \rightarrow 2C + 2H_2$

and $xC \rightarrow$ graphite, CNTs

Hence a small proportion of the hydrogen selectivity is driven by carbon deposition and the formation of graphite and CNTs. This supported by a recent study which showed that the C:H ratio for carbonaceous material deposited during dry reforming was in excess of 100:1 [23]. Note that the hydrogen produced by carbon laydown is not sufficient to make up for the differential observed, nevertheless when no graphite/CNTs were produced (*e.g.* when acetone was the impurity, see below) the hydrogen selectivity is accurately described by the stoichiometric reactions.

Effect of acetone and propyl amine.

The impurities that maintain high ethanol conversion are acetone and propyl amine. Such behaviour has been observed previously with an amine impurity in ESR. Devianto *et al.*[16] and Le Valant *et al.* [17] examined the effect of diethyl amine, among other impurities, on ESR over $Rh/MgAl_2O_4$ and Ni/MgO catalysts respectively and found that the conversion was enhanced. To explain this effect Duprez and co-workers [17] considered that the promotional effect was due to electronic changes in the metal due to electron transfer from the nitrogen. Le Valant *et al.* [17] tested their systems for 8 h and as commented on by Christensen and co-workers [13] it is only over a longer time on stream

that the effects of the impurities will be observed. Our reaction with added propyl amine, as distinct from diethyl amine, does maintain a high activity much longer than the reaction with only ethanol, however by 100 h TOS the conversion of has decreased significantly and is only slightly higher than that with no added impurity. It is clear from the TPO (Fig. 5 and Table 4) that the amount of coke on the catalysts after ESR with the acetone impurity is significantly less than the other systems and slightly reduced when propylamine is the impurity. Indeed the reaction with added acetone gave the least coke (0.09% of the total ethanol feed) and XRD, TEM and Raman spectroscopy confirm that the carbon deposited is not graphitic. Hence the maintenance of high conversion in this case may be related to the change in amount and nature of the carbon deposition. Direct steam reforming of acetone over nickel catalysts has been reported in the literature but there is considerable variation in the results. A study by Sadykov et al. [24] using a Ni/YSZ catalyst modified with Ru reported that during steam reforming acetone deposited more carbon than ethanol and the carbon was more recalcitrant. A similar conclusion was arrived at by Hu and Lu [25], who found that the main carbon deposition sources were carbon monoxide and acetone over a Ni/alumina catalyst, with decomposition or polymerisation being the main routes. In contrast to this is the work of Jensen and co-workers [21], who found that carbon deposition was worse during steam reforming of ethanol and propanol rather than acetone due to the formation of alkenes. A study by Vagia and Lemomidou [26] of acetone steam reforming over a Ni/calcium aluminate catalyst revealed that the support was highly active for the reforming reaction. However we could find no study of acetone steam reforming over a ruthenium catalyst. The selectivities reported in Table 2 and Figs. 2 – 4 for the reactions in the presence of

acetone and propyl amine show lower selectivity to hydrogen than when pure ethanol is used and higher selectivities to methane and carbon dioxide. The selectivity profile observed at 100 h when acetone is present as an impurity can be described by the following reactions:

$$9C_2H_5OH \rightarrow 9CO + 9CH_4 + 9H_2$$

$$5CO + 5H_2O \rightarrow 5CO_2 + 5H_2$$

$$C_2H_5OH \rightarrow C_2H_4 + H_2O$$

Overall: $10C_2H_5OH + 4H_2O \rightarrow 4CO + 9CH_4 + 14H_2 + 5CO_2 + C_2H_4 + H_2O$

While the selectivity profile when propyl amine is the impurity can be described by:

$$4C_2H_5OH \rightarrow 4CO + 4CH_4 + 4H_2$$

$$3CO + 3H_2O \rightarrow 3CO_2 + 3H_2$$

Overall: $4C_2H_5OH + 3H_2O \rightarrow CO + 4CH_4 + 7H_2 + 3CO_2$

In both cases the selectivity can be described principally by ethanol decomposition and the WGS reaction; no steam reforming need be invoked. This is similar to that found with the alumina support. Indeed both the high conversion and reaction selectivity observed from the ESR reactions with acetone and propyl amine as impurities match that found with pure ethanol over the alumina support. No CNTs are found on the alumina after use in ESR with pure ethanol, which is similar to that found when acetone was the impurity in ESR over Ru/alumina. Therefore in the light of these results we propose that acetone and propyl amine induce rapid deactivation of the metal function during ESR and that the residual activity observed is due to the alumina support. Amines are known to be poisons for precious metal catalysts in a variety of reactions [27-30] due to the strong interaction between the nitrogen lone pair and the metal. However in this case the

deactivation of the metal is masked by the conversion associated with the alumina. The difference in the catalyst deactivation can be seen in the change in acetaldehyde yield with TOS is shown in Fig. 9. It is noticeable that with TOS the acetaldehyde yield increases when acetone and propyl amine are the impurities but mildly deactivates when no impurity or 1-propanol is present. It has been shown [31-33] that in ESR ethanol can convert to acetaldehyde and the acetaldehyde can decompose to give carbon monoxide and methane:

$C_2H_5OH \rightarrow CH_3CHO + H_2$

$CH_3CHO \rightarrow CH_4 + CO$

therefore when there is no impurity or another alcohol is present it is the first reaction that is deactivated, whereas in the presence of acetone or propyl amine it is the second

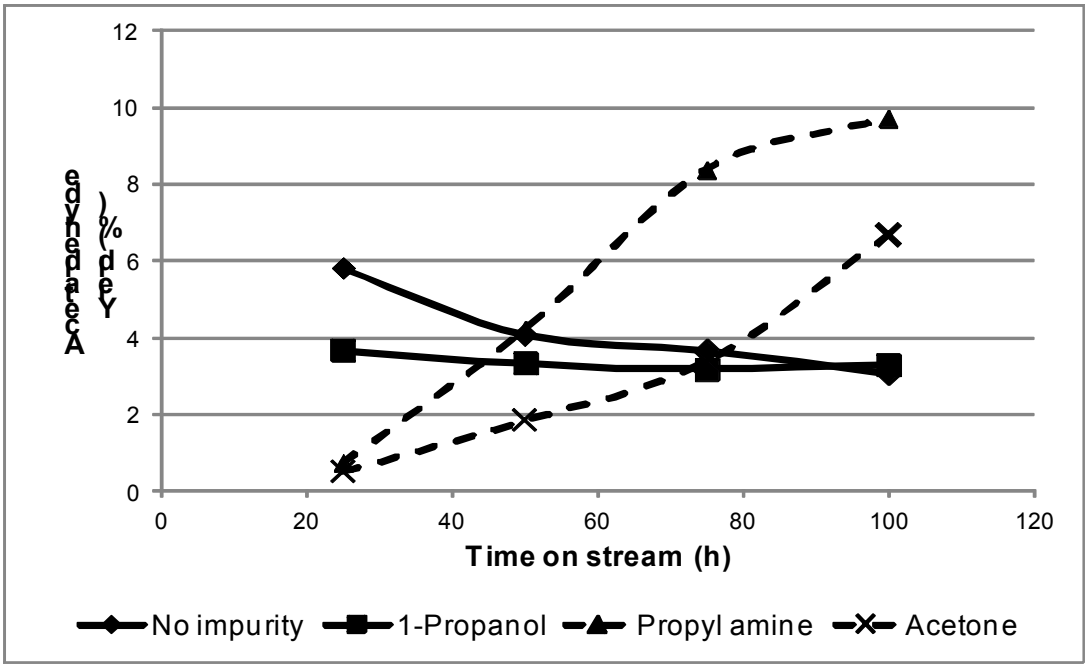

Figure 9. Acetaldehyde yield over Ru/alumina with TOS. Conditions: 773 K, 20 barg, 5:1 water:ethanol, 1 % impurity.

reaction that is deactivated. Further a closer examination of the TPO reveals that the low temperature combustion event occurs approximately 25 K higher in temperature for the catalysts used with both acetone and propyl amine as impurities. This type of carbon deposit has been suggested to be associated with the support [34] however over Ru/Al_2O_3 it was proposed [18] that the metal component was involved, as this material is not present when the alumina is tested in the absence of metal. Therefore the higher temperature needed to combust this carbon when propyl amine and acetone are the impurities may relate to full poisoning of the metal function hence inhibiting the combustion.

Effect of propanal

The behaviour of the ESR system when propanal is added as an impurity is in many ways the most interesting, as at the start of the reaction the selectivity is high to ethene (similar to 1-propanol and IPA) yet by the end of the TOS the selectivity favours methane (similar to that found with acetone and propyl amine). In the first 24 hours TOS the product selectivity can be described by the following reactions:

$$37C_2H_5OH \rightarrow 37C_2H_4 + 37H_2O$$

$$C_2H_4 + H_2 \rightarrow C_2H_6$$

$$5C_2H_5OH \rightarrow 5CO + 5CH_4 + 5H_2$$

$$5CO + 5H_2O \rightarrow 5CO_2 + 5H_2$$

$$1.5C_2H_5OH + 1.5H_2O \rightarrow 3CO + 6H_2$$

giving an ethanol decomposition to ethanol steam reforming ratio of 3.3:1 and an ethanol dehydration to ethanol steam reforming of ~24.5:1. However by 100 h TOS the selectivity is such that although it can be described by the same reactions, the ratios have dramatically changed:

$$7C_2H_5OH \rightarrow 7C_2H_4 + 7H_2O$$

$$C_2H_4 + H_2 \rightarrow C_2H_6$$

$$28C_2H_5OH \rightarrow 28CO + 28CH_4 + 28H_2$$

$$27CO + 27H_2O \rightarrow 27CO_2 + 27H_2$$

$$3.5C_2H_5OH + 3.5H_2O \rightarrow 7CO + 14H_2$$

the ethanol decomposition to ethanol steam reforming ratio is now 8:1, while the ethanol dehydration to ethanol steam reforming ratio has decreased dramatically to 2:1, with the main reaction being ethanol decomposition. Indeed in the first 24 h the reaction system is similar to that observed when IPA was the impurity. Hence there is a clear change in the surface reactions and therefore selectivity as certain active sites are deactivated. Ethanol decomposition becomes the primary reaction, a reaction that can be associated with the support and one that is seen in the absence of metal and when the metal is deactivated. Therefore we suggest that over the course of the 100 h test the metal is deactivated such that by the end of the time on stream the main active component is the support.

Conclusions

The addition of 1 mol.% C-3 based impurities to a water/ethanol mixture had a significant negative effect on the conversion and selectivity of ethanol steam reforming

over a Ru/Al_2O_3 catalyst at 773 K and 20 barg pressure. A summary graph of selectivities is shown in Fig. 10, which shows the very clear difference between the effect

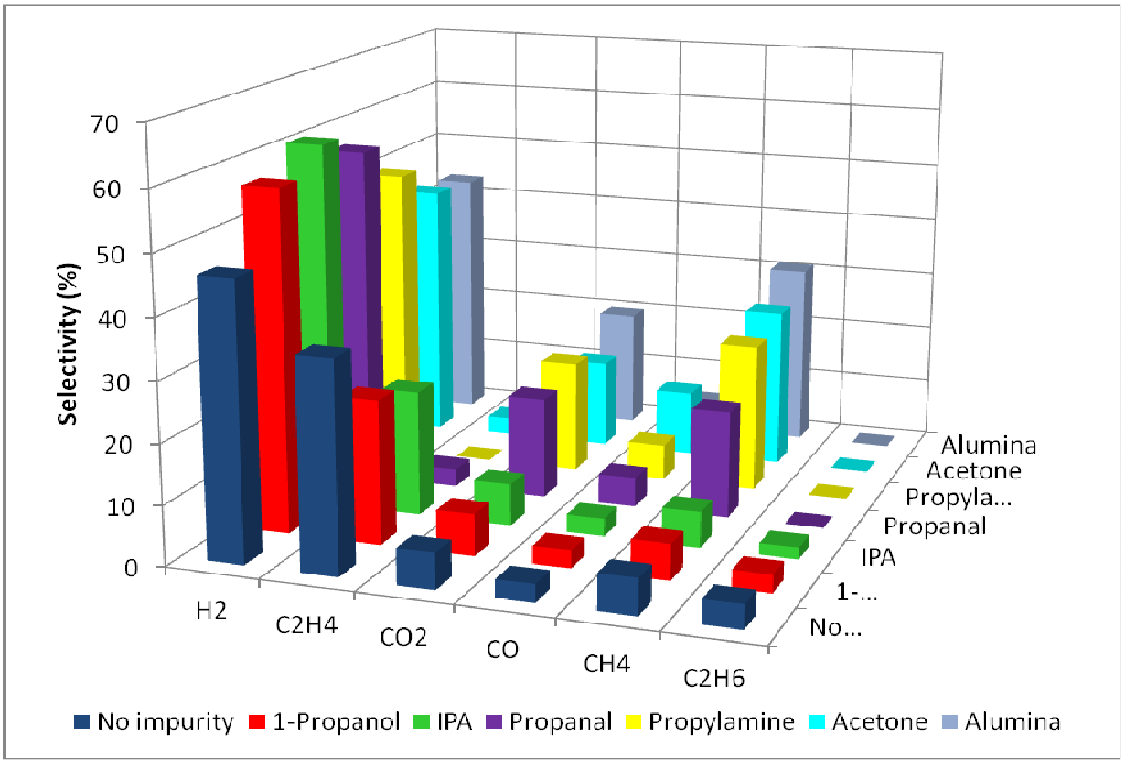

Figure 10. Dry gas molar selectivity at 100 h TOS.

of acetone and propyl amine compared to that of 1-propanol and IPA. The reaction analysis suggests that both propyl amine and acetone rapidly deactivate the metal component of the catalyst and the residual activity relates to that of the alumina support. Whereas 1-propanol and IPA deactivate the catalyst in general affecting both support and metal in a manner similar to the ethanol. The secondary alcohol is more reactive than the primary alcohol with IPA being fully reacted at all TOS. Both propanal and 1-propanol catalyse the formation of CNTs which are not seen in the absence of the impurities. Generating a simple order of the effect of the impurities on the basis of activity gives

acetone > propyl amine > no impurity > IPA > propanal > propanol, an order not that dissimilar that obtained by Duprez and co-workers [17] but if the space time yield of hydrogen is used then the order changes to propyl amine > propanal > acetone > propanol ≈ no impurity > IPA. The amount of carbon monoxide formed may be an issue if the hydrogen product is to be used for a fuel cell application; the order obtained for space time yield of carbon monoxide is acetone > propyl amine > propanal > no impurity > propanol ≈ IPA. So although having a propyl amine impurity can be positive in terms of activity and hydrogen yield it would be poor if low carbon monoxide was required for a fuel cell. If the output of the steam reformer was to be used for hydrogen and ethene then having no impurity gives the highest yield of ethene. Clearly the effect of an impurity is not simple and whether an impurity is acceptable would depend on the application of the steam reformer output. We hope in the future to be able to examine combination effects of impurities.

Acknowledgements

The authors are deeply grateful to Kohat University of Science and Technology Kohat, Pakistan and University of Glasgow, UK for supporting this research.

References

1. H. Cavendish, *Phil. Trans*., 1766, **56,** 141-184.

2. G. Maxwell, *Synthetic Nitrogen Products A Practical Guide to the Products and Processes*, Springer US, New York, 2005, pp. 47-162.

3. C. H. Bartholomew, R. J. Farrauto, *Fundamentals of Industrial Catalytic Processes, 2nd ed.*, John Wiley and Sons, New Jersey, 2006.

4. K. Takanabe, K.-I. Aika, K. Inazu, T. Baba, K. Seshan, L. Lefferts, *J. Catal*., 2006, **243**, 263-269.

5. U.S. Department of Energy Report, *Report of the Hydrogen Production Expert Panel to HTAC*, 2013.

6. O. Gorke, P. Pfeifer, K. Schubert, *Appl. Catal. A*, 2009, **360**, 232-241.

7. A. Haryanto, S. Fernando, N. Murali, S. Adhikari, *Energy Fuels*, 2005, **19**, 2098-2106.

8. N. Meng, M.K.H. Leung, K. Sumathy, D.Y.C. Leung, *Int. J. Hydrogen Energy*, 2006, **31**, 1401-1412.

9. K. Balat, E. Kirtay, *Int. J. Hydrogen Energy,* 2010, **35**, 7416-7426.

10. G. Wen, Y. Xu, H. Ma, Z. Xu, Z. Tian, *Int. J. Hydrogen Energy*, 2008, **33**, 6657-6666.

11. N. Bion, F. Epron, D. Duprez, *Catalysis*, 2010, **22**, 1–55

12. M. Benito, J. L. Sanz, R. Isabel, R. Padilla, R. Arjona, L. Daza, *J. Power Sources*, 2005, **151**, 11-17.

13. J. Rass-Hansen, R. Johansson, M. Moller, C. H. Christensen, *Int. J. Hydrogen Energy*, 2008, **33**, 4547-4554.

14. A. Le-Valant, F. Can, N. Bion, D. Duprez, F. Epron, *Int. J. Hydrogen Energy*, 2010, **35**, 5015-5020.

15. M. R. Ladisch, K. Dyck, *Science*, 1979, **205**, 898-900.

16. H. Devianto, J. Han, S. P. Yoon, S. W. Nam, T.-H. Lim, I.-H. Oh, S.-A. Hong, H.-I. Lee, *Int. J. Hydrogen Energy*, 2011, **36**, 10346-10354

17. A. Le-Valant, A. Garron, N. Bion, F. Epron, D. Duprez, *Catal. Today,* 2008, **138**, 169-174.

18. M. Bilal, S. D. Jackson, *Catal. Sci. Technol*., 2012, **2**, 2043-2051

19. J. R. Rostrup-Nielsen, J.-H. B. Hansen, *J. Catal*. 1993, **144**, 38-49

20. K. Aasberg-Petersen, I. Dybkjær, C. V. Ovesen, N. C. Schjødt, J. Sehested, S. G. Thomsen, *J. Natural Gas Sci. Eng*., 2011, **3**, 423-459

21. R. Trane-Restrup, D. E. Resasco, A. D. Jensen, *Catal. Sci. Technol*., 2013, **3**, 3292-3302

22. J. R. Rostrup-Nielsen, J. Sehested, J. K. Nørskov, *Adv. Catal*., 2002, **47**, 65–139

23. I. P. Silverwood, N. G. Hamilton, C. J. Laycock, J. Z. Staniforth, R. M. Ormerod, C. D. Frost, S. F. Parker, D. Lennon, *Phys. Chem. Chem. Phys*., 2010, **12**, 3102–3107

24. V. Sadykov, N. Mezentseva, G. Alikina, R. Bunina, V. Rogov, T. Krieger, S. Belochapkine, J. Ross, *Catal. Today*, 2009, **145**, 127–137

25. X. Hu, G. Lu, *Appl. Catal. B*, 2009, **88**, 376–385

26. E. Ch. Vagia, A. A. Lemonidou, *Appl. Catal. A*, 2008, **351**, 111–121

27. K. F. Graham, K. T. Hindle, S. D. Jackson, D. J. M. Williams, S. Wuttke, *Top. Catal*., 2010, **53**, 1121–1125

28. E. L. Pitara, B. N'Zemba, J. Barbier, F. Barbot, F. Miginiac, *J. Mol Catal A*, 1996, **106**, 235

29. C. H. Bartholomew, *Appl. Catal. A*, 2001, **212**, 17–60

30. P. Albers, J. Pietsch, S. F. Parker, *J. Mol. Catal. A*, 2001, **173**, 275-286

31. M. Benito, J. L. Sanz, R. Isabel, R. Padilla, R. Arjona, L. Daza, *J. Power Sources*, 2005, **151**, 11–17

32. G. Jacobs, R. A. Keogh, B. H. Davis, *J Catal*., 2007, **245**, 326–337

33. H. Song, L. Zhang, U. S. Ozkan, *Ind. Eng. Chem. Res*., 2010, **49**, 8984–8989

34. F. Can, A. Le-Valant, N. Bion, F. Epron, D. Duprez, *J. Phys. Chem. C*, 2008, **112**, 14145-14153